2025 年 第 25 卷 第 22 期
2025, 25(22): 09260-13

科 学 技 术 与 工 程
Science Technology and Engineering

ISSN 1671—1815
CN 11—4688/T

DOI: 10.12404/j.issn.1671-1815.2407159
引用格式: 张文斌, 赵振琯, 何碧, 等. 北山南带长山二长花岗岩年代学、地球化学特征及其地质意义[J]. 科学技术与工程, 2025, 25(22): 9260-9272.
Zhang Wenbin, Zhao Zhengguan, He Bi, et al. Geochronology, geochemistry characteristics and tectonic significance of Changshan monzogranite in the southern Beishan belt[J]. Science Technology and Engineering, 2025, 25(22): 9260-9272.

北山南带长山二长花岗岩年代学、地球化学特征及其地质意义

张文斌, 赵振琯, 何碧, 王宁祖, 吴浩博, 张志玺
(甘肃省地质矿产勘查开发局第二地质矿产勘查院, 兰州 730000)

摘 要 甘肃北山南带位于中亚造山带南部,是研究中亚造山带构造演化的重要区域,其晚古生代构造背景争议已久。为进一步探讨北山南带晚古生代构造演化,选取北山南带长山二长花岗岩体为对象,分析了其年代学和地球化学特征。研究发现二长花岗岩的 LA-ICP-MS 锆石 U-Pb 加权平均年龄为(291.1±1.5)Ma,形成于早二叠世。地球化学数据显示,岩体为过铝质钙碱性高钾-钾玄质系列。SiO_2 含量为 72.07%~72.94%,K_2O 含量为 4.93%~5.10%,且 $K_2O > Na_2O$,Al_2O_3 含量为 13.52%~13.97%。稀土元素球粒陨石标准化曲线呈右倾,轻稀土相对富集(LREE/HREE 为 10.96~14.98),δEu 为 0.78~0.92,具弱负 Eu 异常。微量元素相对富集大离子亲石元素、贫化高场强元素,显著亏损高场强元素 Nb、Sm、Y。根据区域构造演化及岩石学、地球化学等特征,认为其是后碰撞过程岩浆活动的产物,反映出中亚造山带南缘碰撞拼贴早于早二叠世完成。

关键词 北山南带; 早二叠世; 二长花岗岩; 锆石定年
中图法分类号 P595 P581; **文献标志码** A

Geochronology, Geochemistry Characteristics and Tectonic Significance of Changshan Monzogranite in the Southern Beishan Belt

ZHANG Wen-bin, ZHAO Zheng-guan, HE Bi, WANG Ning-zu, WU Hao-bo, ZHANG Zhi-xi
(The Second Institute of Geology and Minerals Exploration, Gansu Provincial Bureau of Geology and Minerals Exploration and Development, Gansu, Lanzhou 730000, China)

[**Abstract**] Located in the south of the Central Asian orogenic belt, the southern Beishan belt in Gansu Province is a key area for studying the tectonic evolution of the Central Asian orogenic belt. Its late Paleozoic tectonic setting has been controversial for a long time. In order to further explore the late Paleozoic tectonic evolution of the southern Beishan belt, the geochronology and geochemical characteristics of the Changshan monzogranite body were analyzed. The analysis results show that the LA-ICP-MS zircon U-Ph weighted average age of the Changshan monzogranite is (291.1±1.5) Ma, and the emplacement of the plutons occurred in the early Permian. Geochemical datas show that the plutons are high potassium calc-alkaline and peraluminous series rocks. The results show that SiO_2 ranges from 72.07% to 72.94%, K_2O ranges from 4.93% to 5.10%, and the contents of $K_2O > Na_2O$, Al_2O_3 ranges from 13.52% to 13.97%. The curves of chondrite-normalized REE are obviously right inclined, and the LREE are relatively enriched (LREE/HREE are 10.96~14.98), δEu are 0.78~0.92, with weak negative Eu anomaly. Trace elements are relatively enriched in LILE (large ion lithophile elements), depleted HFSE (high field strength elements), and significantly depleted in high field strength Elements Nb, Sm, Y. According to the regional tectonic setting, petrological and geochemical characteristics, the Changshan adamellite plutons are considered to be the product by post-collisional magmatic activity, reflecting the completion of the collision collage on the southern margin of the Central Asian orogenic belt in the early Permian.

[**Keywords**] the Beishan southern belt; Early Permian; monzogranite; Zircon dating

中亚造山带位于塔里木板块、西伯利亚板块结合部位[1-2],其南缘构造演化及古亚洲洋的闭合时间一直是争议的焦点[2-8]。相关研究结果表明,北山南带地区洋盆闭合于晚二叠世[9-11];也有一些研

收稿日期: 2024-09-25; **修订日期**: 2025-05-13
基金项目: 甘肃省自然资源厅科技创新项目(202413);甘肃省自然科学基金(25JRRA392,24JRRA752);甘肃省地质矿产勘查开发局科技创新项目(2024KS02);甘肃省基础地质调查项目(甘财资环〔2020〕90 号,甘财资环〔2021〕77 号)
第一作者: 张文斌(1983—),男,汉族,新疆昌吉人,高级工程师。研究方向:区域地质与矿产勘查。E-mail: zhangwbhcx2023@163.com。

究者认为该区洋盆闭合于志留纪末—泥盆纪初[12]、石炭纪[13]、早二叠世前[14]、中三叠世时期[15],部分学者认为红柳园一带枕状玄武岩形成于深海盆地或裂谷环境[16]。因此,对北山南带晚古生代构造环境的认识一直存在争议[17-18],限制了对中亚造山带的整体认识。红柳河—牛圈子—洗肠井蛇绿岩带将北山造山带分为北带和南带[19-22]。

北山南带岩浆活动强烈,花岗岩分布广泛,以海西期花岗岩为主,众多学者对北山南带海西期花岗岩开展了较深入的研究,探讨了其形成的构造背景及源区性质,其中泥盆纪北山南带主要受俯冲作用[20,23-25],石炭纪—二叠纪进入后碰撞演化阶段,但就具体时限争议较大[26-32]。同时对岩浆岩的源区性质及其岩浆作用过程也存在争议,有幔源成因、壳幔混源等[32-33]。

长山二长花岗岩体位于北山南带南缘,目前尚未对其开展过年代学及岩石地球化学研究。现选择北山南带长山二长花岗岩体开展研究,综合应用岩相学、LA-ICP-MS 锆石 U-Pb 年代学测定、岩石主微量元素测定等方法进行分析,探讨其岩石地球化学特征及其成岩年代,恢复其成岩环境;为北山地区古洋盆闭合、碰撞造山时限等洋—陆构造格局及其演化问题提供新的地质依据。

1　地质背景

北山长山地区位于中亚造山带之北山造山带[31][图 1(a)],北山造山带是在长期的板块碰撞和地质演化基础上形成[19,34],分布有 4 条蛇绿岩带,为红石山蛇绿混杂岩带、明水—石板井—小黄山蛇绿混杂岩带、红柳河—牛圈子—洗肠井蛇绿混杂岩带、柳园—账房山蛇绿混杂岩带[9-10,20,31],如图 1(b)所示。

北山南带岩浆岩十分发育,以海西期岩浆岩分布最为广泛,为研究北山南带晚古生代构造演化提供了重要的载体。前人对海西期花岗岩构造属性开展了一定的研究,江思宏等[35]认为北山南带海西晚期(310 ~ 270 Ma)为同碰撞环境;杨镇熙等[36]通过对黑山头石英二长闪长岩(267.7 ± 1.3)Ma 构造属性研究,认为北山南带中二叠世已完成洋—陆构造转化,进入后碰撞板内裂谷演化阶段;冯继承等[37]认为桥湾北岩体(303.7 ± 2.4) Ma 是北山南带后碰撞过程岩浆活动的产物;孙海瑞等[31]认为柳园地区早二叠世正长花岗斑岩脉(288.5 ± 1.4) Ma 形成于俯冲作用过程中的局部伸展环境,同碰撞环境至少持续到早二叠世;赵宏刚等[32]认为北山南带沙枣园复式岩体(252.1 ± 1.9) Ma 形成于俯冲—碰撞构造背景下,至印支早期(246.4 ± 2.0) Ma 转变为碰撞后构造背景,上述研究表明北山南带的花岗岩成因仍存在争议。

研究区位于石板山岛弧带,区内侵入岩十分发育,主要有晚石炭世斑状花岗岩、早石炭世石英二长岩、早二叠世二长花岗岩,发育闪长玢岩脉、弧状展布的花岗斑岩脉;区内断裂构造主要为北东向及近东西向平移断层[图 1(c)]。

2　岩石学特征

长山二长花岗岩体呈北西向分布于甘肃省瓜州县长山一带,面积 6.27 km^2,其北东侧侵入于石英二长岩,南西侧侵入于晚石炭世斑状花岗岩[图 1(c)]。

岩石呈浅肉红色[图 2(a)],块状构造[图 2(b)],中细粒花岗结构;主要矿物:石英(28% ±):他形粒状,粒度为 0.05 ~ 1.85 mm,见少量石英晶体与长石构成文象结构;斜长石(40% ±):半自形-自形板状,长径为 0.10 ~ 2.20 mm,绢云母化相对较强,发育聚片双晶和环带构造;钾长石(28% ±):他形粒状,主要为条纹长石,粒度 0.10 ~ 2.00 mm,客晶呈焰火状、水滴状分布;黑云母(3% ±):鳞片状,长径 0.05 ~ 0.60 mm,部分黑云母沿边缘和解理绿泥石化、高岭土化、葡萄石化微弱;角闪石(1% ±):呈半自形粒状,粒径 0.01 ~ 0.12 mm,发育绿泥石化;副矿物为锆石、电气石、榍石等[图 2(c)]。

3　锆石 U-Pb 测年结果

3.1　分析方法

本次工作在长山地区二长花岗岩岩体采集了 1 件锆石 U-Pb 测年样品,采集处无后期蚀变,采集过程排除和避免外来物质的污染。在广州市拓岩检测技术有限公司完成测试分析,主要包括锆石的挑选、制靶、拍照、图像分析以及 U-Pb 定年测试等。选择的实验设备为 NWR 激光剥蚀系统,ICP-MS。设置激光频率为 6 Hz,能量密度 3.5 J/cm^2。标准锆石 Plešovice 为盲样。采集的信号中有 30 s 空白信号和 40 s 样品信号。通过 ICPMSDataCal 工具对数据离线处理,为后续分析提供支持。

3.2　分析结果

阴极发光影像结果表明,采集的锆石大部分为无色透明,自形-半自形长柱状,形态完整、晶型较好、粒径大(150 ~ 230 μm),长宽比在 1 ~ 3,具有典型的岩浆成因韵律环带构造[38-39],如图 3 所示。样品共测试了 44 颗锆石的 44 个测点,分析结果如表 1 所示;$w(\mathrm{U}) = 91.99 \times 10^{-6} \sim 368.62 \times 10^{-6}$,$w(\mathrm{Th}) = 57.96 \times 10^{-6} \sim 227.02 \times 10^{-6}$,Th/U = 0.53 ~

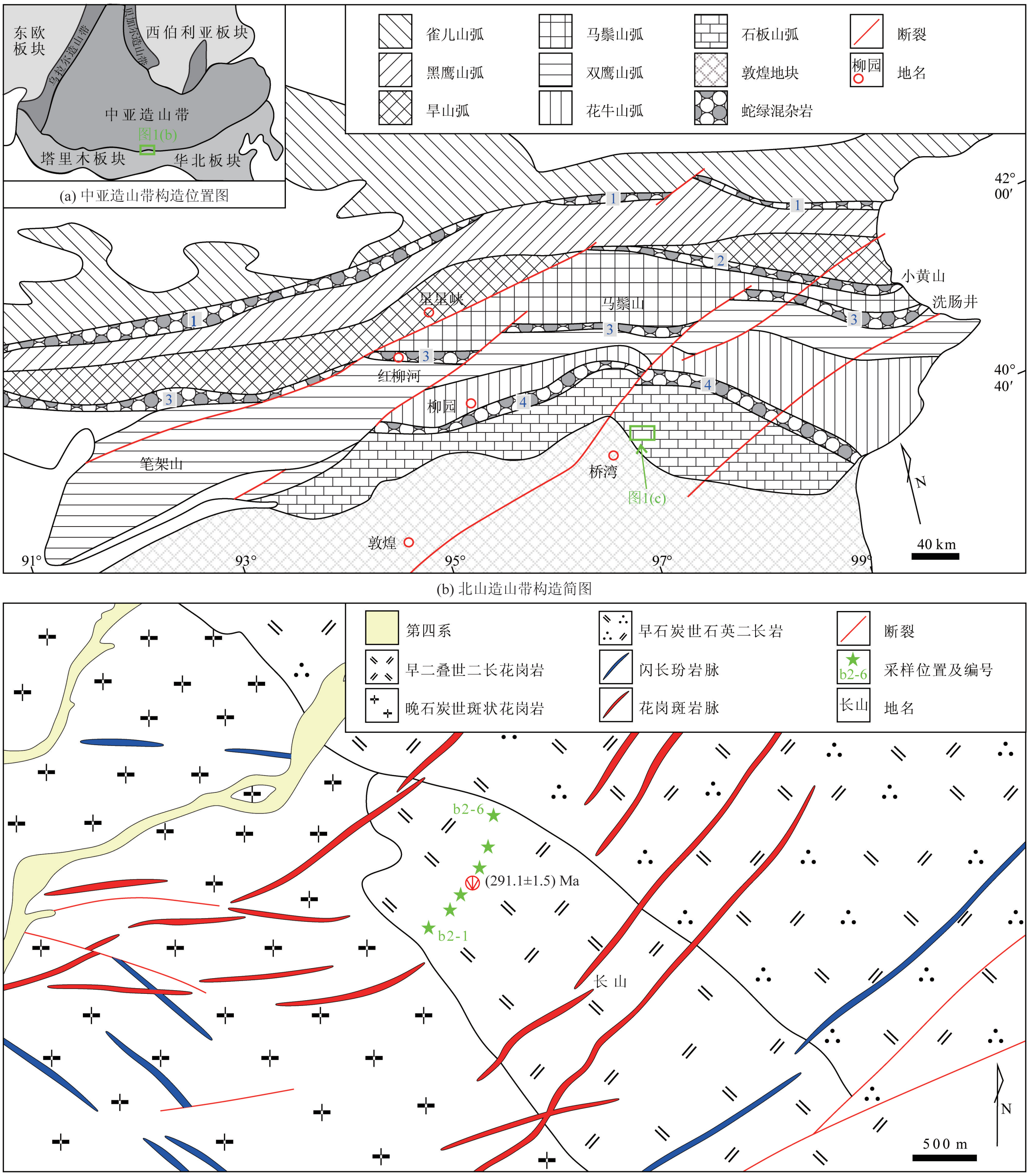

(b) 北山造山带构造简图

(c) 长山地区地质简图

1 为红石山蛇绿混杂岩带;2 为明水-石板井-小黄山蛇绿混杂岩带;3 为红柳河-牛圈子-洗肠井蛇绿混杂岩带;4 为柳园-账房山蛇绿混杂岩带

图 1 中亚造山带构造位置图[31]、北山造山带构造简图[31]及长山地区地质简图

Fig. 1 Structural location map of Central Asia orogenic belt[31], structural sketch map of Beishan orogenic belt[31] and geological sketch map of Changshan area

1.06,大于 0.1,指示为岩浆成因锆石[40]。44 个测点的U-Pb年龄一致性高,样品获得$^{206}Pb/^{238}U$ 年龄在 $^{206}Pb/^{238}U-^{207}Pb/^{235}U$ 谐和年龄图中[图 4(a)]。所有测点都分布于谐和线附近或线上,谐和度为 93% ~99%,锆石的谐和年龄为(292.14 ± 0.48) Ma,MSWD = 3.9。其$^{206}Pb/^{238}U$ 年龄的加权平均值为(291.1 ±1.5) Ma[图 4(b)],岩体就位年龄为早二叠世。

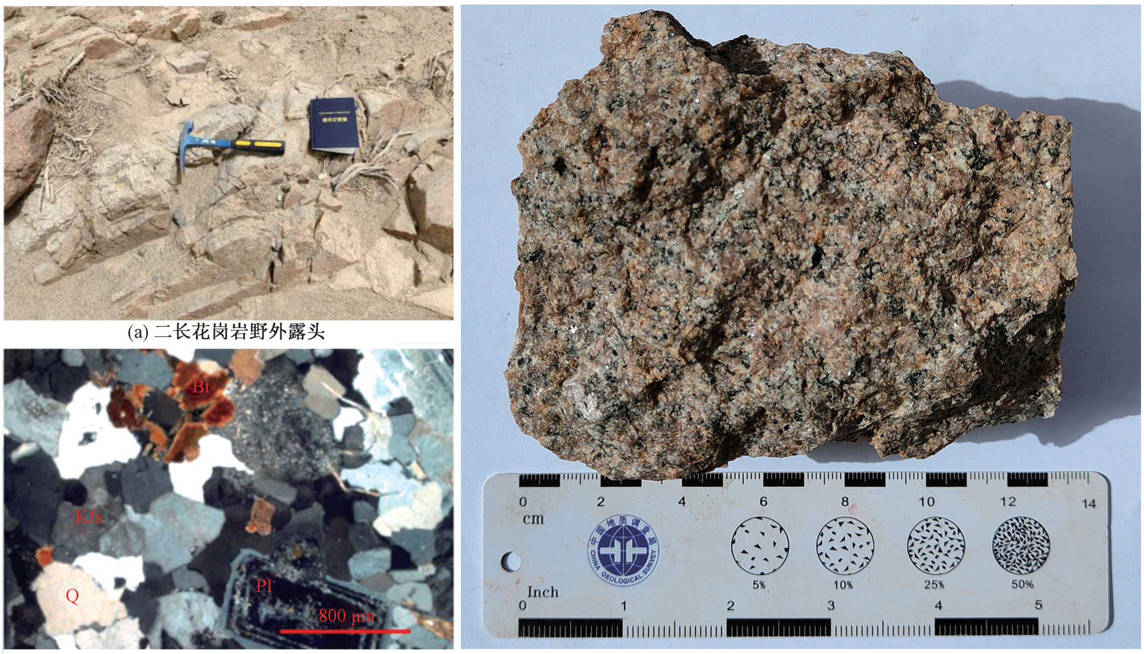

(a) 二长花岗岩野外露头

(c) 二长花岗岩显微特征　　(b) 二长花岗岩标本

Bt 为黑云母;Kfs 为钾长石;Q 为石英;Pl 为斜长石

图 2　长山二长花岗岩野外露头及正交偏光显微特征

Fig. 2　Field outcrops of monzonitic granite and microscopic characteristics

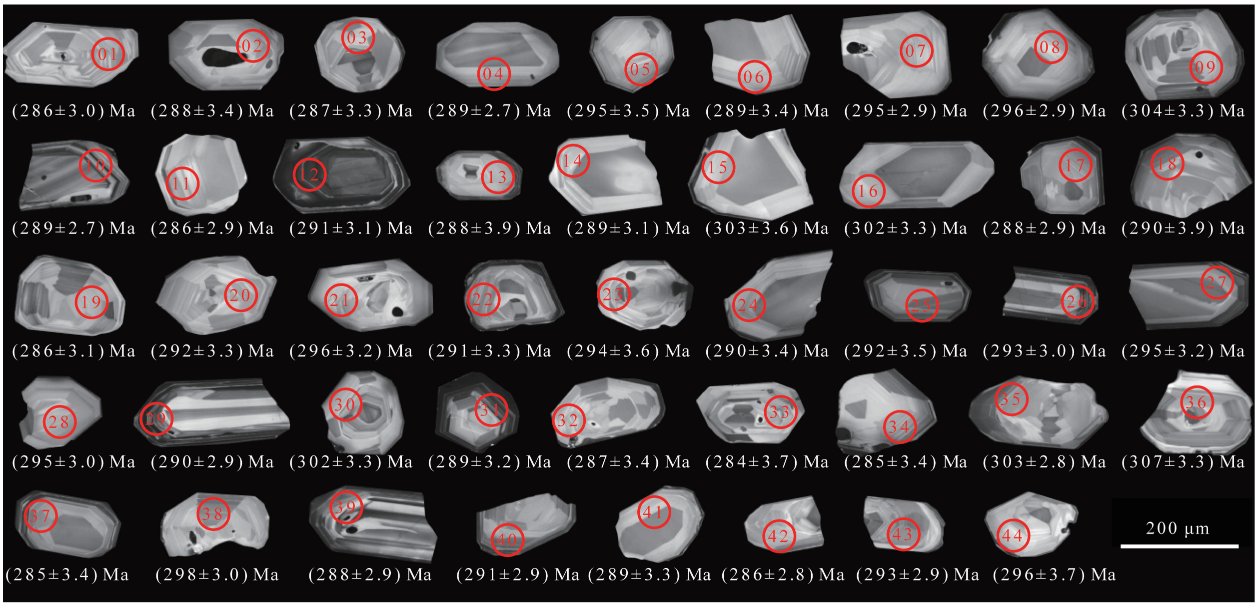

图 3　长山二长花岗岩锆石特征和测点位置

Fig. 3　Characteristics and dating spots of zircons from Changshan monzogranite

表 1　长山二长花岗岩 LA-ICP-MS 锆石 U-Pb 同位素分析结果

Table 1　U-Pb dating data of granite LA-ICP-MS in Changshan monzogranite

样品编号	同位素比值				同位素年龄/Ma				同位素含量/10^{-6}		
	$^{207}Pb/^{235}U$	σ	$^{206}Pb/^{238}U$	σ	$^{207}Pb/^{235}U$	σ	$^{206}Pb/^{238}U$	σ	Th	U	Pb
1	0. 335 0	0. 013 5	0. 045 4	0. 000 5	293	10	286	3	82. 80	116. 81	6. 46
2	0. 332 3	0. 014 5	0. 045 8	0. 000 6	291	11	289	3	65. 75	100. 30	5. 57
3	0. 333 8	0. 012 6	0. 045 5	0. 000 5	293	10	287	3	87. 08	123. 76	6. 83
4	0. 312 0	0. 012 8	0. 045 8	0. 000 4	276	10	289	3	82. 02	111. 08	6. 32
5	0. 342 4	0. 014 2	0. 046 7	0. 000 6	299	11	295	4	57. 96	91. 99	5. 09
6	0. 340 2	0. 012 3	0. 045 9	0. 000 5	297	9	290	3	144. 30	164. 06	9. 62
7	0. 339 8	0. 009 9	0. 046 8	0. 000 5	297	8	295	3	140. 95	236. 99	13. 07

续表 1

样品编号	同位素比值				同位素年龄/Ma				同位素含量/10^{-6}		
	$^{207}Pb/^{235}U$	σ	$^{206}Pb/^{238}U$	σ	$^{207}Pb/^{235}U$	σ	$^{206}Pb/^{238}U$	σ	Th	U	Pb
8	0.350 1	0.016 4	0.047 0	0.000 5	305	12	296	3	89.46	119.23	6.86
9	0.350 7	0.011 5	0.048 3	0.000 5	305	9	304	3	200.98	288.86	16.54
10	0.337 9	0.011 2	0.045 8	0.000 4	296	9	289	3	112.21	157.47	8.73
11	0.344 9	0.014 7	0.045 3	0.000 5	301	11	286	3	79.21	117.47	6.36
12	0.328 4	0.011 9	0.046 2	0.000 5	288	9	291	3	92.82	149.02	8.07
13	0.326 9	0.011 7	0.045 6	0.000 6	287	9	288	4	72.02	113.54	6.13
14	0.328 9	0.010 7	0.045 8	0.000 5	289	8	289	3	109.42	168.87	9.18
15	0.342 8	0.010 3	0.048 2	0.000 6	299	8	303	4	181.33	339.54	18.42
16	0.331 1	0.012 4	0.047 9	0.000 5	290	10	302	3	140.83	209.33	11.74
17	0.333 2	0.007 7	0.045 8	0.000 5	292	6	288	3	225.74	368.62	19.47
18	0.330 2	0.016 5	0.046 1	0.000 6	290	13	290	4	64.73	92.44	5.10
19	0.319 1	0.011 8	0.045 3	0.000 5	281	9	286	3	129.73	160.10	8.91
20	0.339 8	0.014 5	0.046 4	0.000 5	297	11	292	3	87.22	126.47	7.05
21	0.331 6	0.013 3	0.046 9	0.000 5	291	10	296	3	83.17	116.35	6.52
22	0.354 1	0.012 7	0.046 2	0.000 5	308	10	291	3	66.16	99.24	5.46
23	0.355 9	0.014 9	0.046 7	0.000 6	309	11	294	4	108.09	132.70	7.67
24	0.356 1	0.013 0	0.046 0	0.000 6	309	10	290	3	113.19	146.31	8.24
25	0.330 0	0.017 8	0.046 3	0.000 6	290	14	292	3	66.55	111.14	6.06
26	0.322 2	0.009 7	0.046 5	0.000 5	284	7	293	3	161.38	250.19	13.69
27	0.361 1	0.013 7	0.046 9	0.000 5	313	10	295	3	85.54	128.66	7.07
28	0.333 0	0.012 0	0.046 9	0.000 5	292	9	295	3	182.78	208.91	12.16
29	0.352 8	0.012 6	0.046 0	0.000 5	307	10	290	3	88.53	152.94	8.24
30	0.334 0	0.010 2	0.047 9	0.000 5	293	8	302	3	125.15	193.95	10.89
31	0.324 5	0.014 4	0.045 9	0.000 5	285	11	289	3	94.89	135.99	7.47
32	0.348 2	0.011 7	0.045 5	0.000 6	303	9	287	3	106.88	168.29	9.12
33	0.338 4	0.016 0	0.045 1	0.000 6	296	12	284	4	115.19	150.44	8.32
34	0.308 2	0.014 9	0.045 2	0.000 5	273	12	285	3	68.11	107.50	6.09
35	0.340 5	0.010 4	0.048 2	0.000 5	298	8	303	3	129.68	165.20	9.82
36	0.329 0	0.011 2	0.048 8	0.000 5	289	9	307	3	117.76	169.32	10.09
37	0.327 6	0.015 3	0.045 2	0.000 6	288	12	285	3	105.05	124.69	7.22
38	0.363 3	0.011 6	0.047 4	0.000 5	315	9	298	3	178.33	205.46	12.19
39	0.325 9	0.011 8	0.045 7	0.000 5	286	9	288	3	105.69	145.23	8.16
40	0.349 3	0.010 2	0.046 2	0.000 5	304	8	291	3	140.79	173.81	10.22
41	0.320 0	0.011 7	0.045 8	0.000 5	282	9	289	3	100.82	134.41	7.65
42	0.339 4	0.011 9	0.045 3	0.000 5	297	9	286	3	97.03	117.41	6.70
43	0.351 6	0.014 5	0.046 5	0.000 5	306	11	293	3	94.21	121.86	7.01
44	0.355 1	0.011 7	0.047 0	0.000 6	309	9	296	4	227.02	213.66	13.20

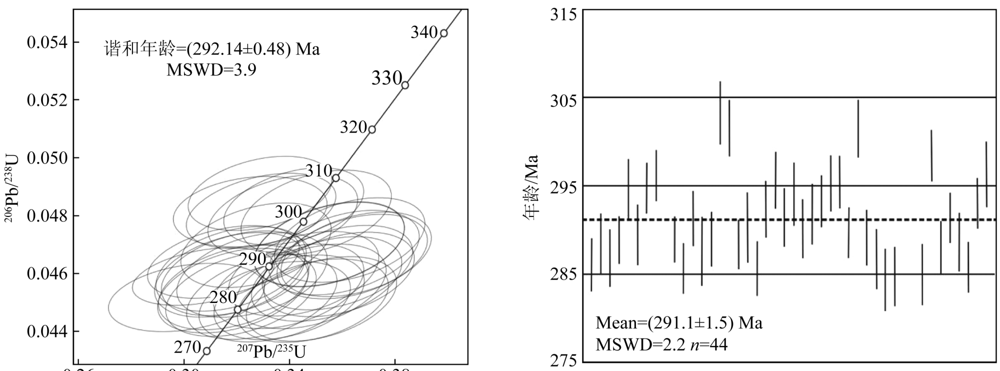

(a) 锆石U-Pb谐和年龄　　(b) 锆石U-Pb加权平均值年龄

图 4　长山二长花岗岩锆石 U-Pb 谐和图和加权平均年龄图

Fig. 4　Zircon U-Pb concordia and weighted average age diagrams of the Changshan monzogranite

4　地球化学特征

4.1　分析方法

本次工作在长山地区二长花岗岩体采集了 6 件样品,样品编号为 b2-1 ~ b2-6,图 1(c)显示出采样地点分布情况。采集的样品在广州市拓岩公司内检测。样品中稀土和微量元素含量通过 ICP-MS 方法测量,主量元素则通过 X 荧光光谱玻璃熔片法检测。

4.2　主量元素

长山地区二长花岗岩主量元素结果如表 2 所示。长山二长花岗岩具有高硅富钾、低铝低镁的特征。SiO_2 含量为 72.07% ~ 72.94%,平均为 72.71%;K_2O 含量为 4.93% ~ 5.10%,平均为 5.03%;Na_2O 含量为 2.40% ~ 2.55%,平均为 2.49,$K_2O/Na_2O > 1$;Al_2O_3 含量为 13.52% ~ 13.97%,平均为 13.73%;MgO 含量为 0.53% ~ 0.58%,平均为 0.56%,$Mg^{\#}$为 20.79 ~21.69;CaO 含量为1.50% ~1.69%,平均为1.61%。

在花岗岩 R1-R2 图解中所有的样品均落入二长花岗岩区[图 5(a)];碱度率(AR)为 1.93 ~ 2.00,平均值为1.96,碱性计算值为0.54 ~0.55,平均0.55,均小于0.9,在 AR-SiO_2图中,全部样品均落入钙碱性区域[图5(b)],为钙碱性花岗岩;在 SiO_2-K_2O 图解中,大多数样品均落入钾玄岩系列,如图5(c)所示;A/CNK-A/NK 图解中,样品均落入过铝质区域,为过铝质岩系列[图5(d)]。综合主量元

表 2　长山二长花岗岩主量元素分析结果

Table 2　Analytical results of major elements of the Changshan monzogranite

主量元素	含量/%					
	b2-1	b2-2	b2-3	b2-4	b2-5	b2-6
SiO_2	72.64	72.82	72.07	72.90	72.94	72.92
Na_2O	2.48	2.40	2.53	2.55	2.50	2.47
MgO	0.58	0.55	0.57	0.55	0.53	0.58
Al_2O_3	13.92	13.57	13.97	13.85	13.58	13.52
P_2O_5	0.05	0.04	0.05	0.05	0.05	0.05
K_2O	5.10	5.04	5.03	5.06	5.02	4.93
CaO	1.61	1.58	1.69	1.50	1.62	1.65
TiO_2	0.22	0.20	0.21	0.21	0.20	0.21
MnO	0.03	0.03	0.02	0.02	0.03	0.02
$Fe_2O_3^T$	2.11	2.02	2.08	2.02	2.03	2.13
LOI	1.06	1.10	1.05	1.13	1.01	0.93
AR	1.94	1.93	1.96	2.00	1.98	1.97
A/CNK	1.12	1.12	1.11	1.13	1.10	1.10
A/NK	1.45	1.44	1.45	1.43	1.42	1.44
R1	2 774	2 847	2 750	2 778	2 816	2 844
R2	481	471	493	466	474	478
$Mg^{\#}$	21.69	21.36	21.55	21.48	20.79	21.30
碱性	0.54	0.55	0.54	0.55	0.55	0.55

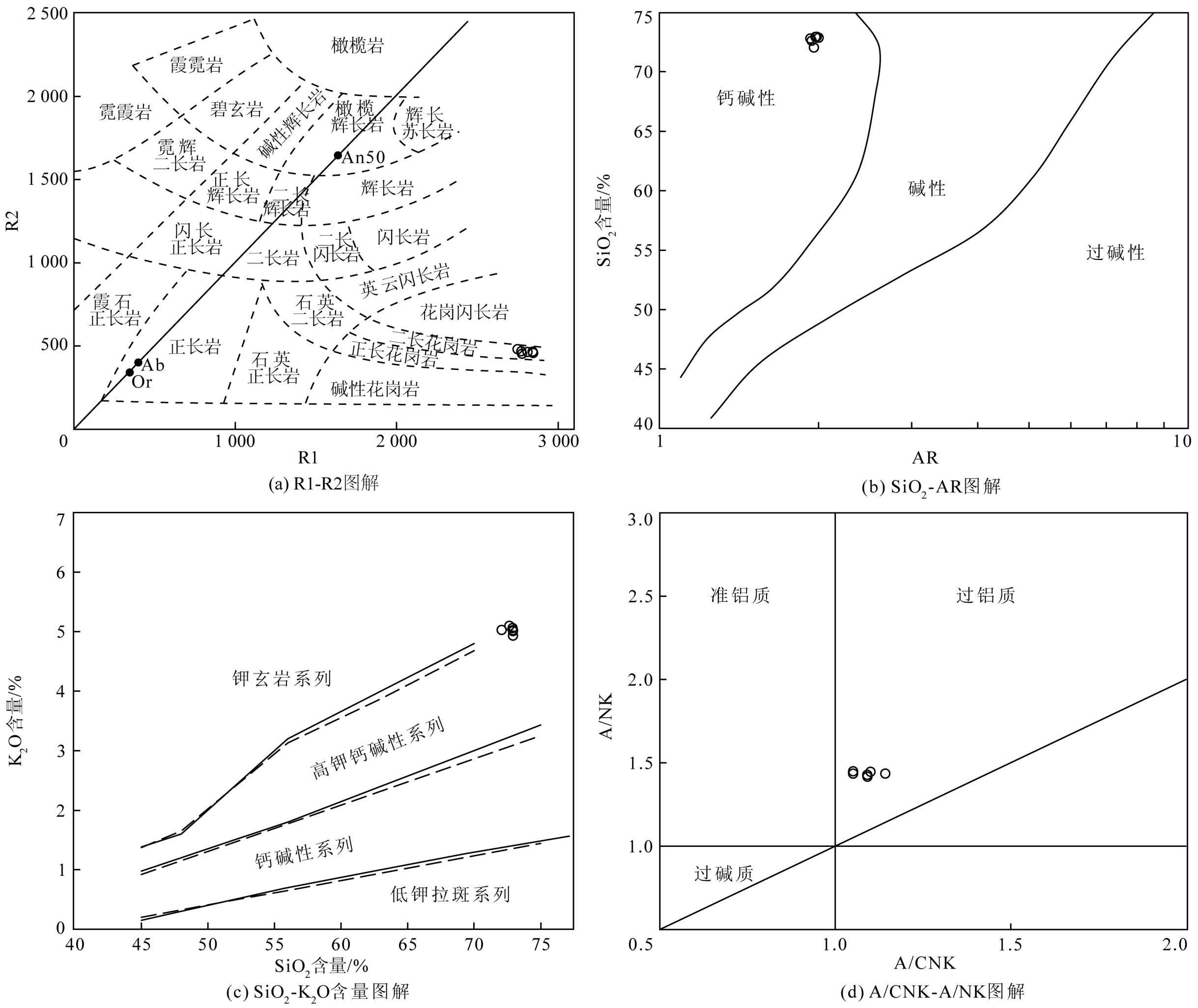

图5　主量元素地球化学图解[41-44]

Fig. 5　Geochemical diagrams of major elements of the Changshan monzogranite[41-44]

素含量相关数据,长山二长花岗岩属于过铝质钙碱性高钾-钾玄质系列岩石。

4.3 稀土、微量元素

稀土及微量元素分析结果如表3所示,稀土总量中等且变化不大(ΣREE 均值为 116.36×10^{-6}),轻重稀土分馏中等偏弱(La_N/Yb_N均值为13.49),铕显示弱负异常(δEu=0.78~0.92,平均为0.83),说明岩浆演化过程中存在一定程度的斜长石的结晶分离或源区斜长石的残留[45];LREE 富集,HRFF 亏损的且平滑或轻微上凹的右倾,弱负铕异常的稀土模式[图6(a)]。微量元素相对富集大离子亲石元素(LILE)、贫化高场强元素(HFSE)且显著亏损高场强元素 Nb、Sm、Y[图6(b)]。

表3 长山二长花岗稀土元素及微量元素分析结果

Table 3 Analytical results of rare earth element and trace elements of the Changshan monzogranite

元素	含量/10^{-6}					
	b2-1	b2-2	b2-3	b2-4	b2-5	b2-6
Ba	659.00	598.00	699.00	634.00	614.00	587.00
Rb	162.00	163.00	163.00	167.00	166.00	173.00
Sr	276.00	258.00	282.00	286.00	266.00	268.00
Zr	121.00	122.00	121.00	128.00	116.00	136.00
Nb	11.50	12.50	9.91	9.53	12.80	9.47
Ni	0.84	0.88	1.53	0.51	25.10	1.43
Co	4.54	4.53	4.20	4.44	4.22	5.72
Zn	25.70	20.70	17.10	17.40	18.60	16.40
Cr	2.81	3.21	3.36	2.36	4.79	3.22
La	28.60	25.30	28.10	29.10	25.70	30.10
Ce	53.90	48.80	55.10	58.20	47.40	56.70
Pr	5.76	5.04	5.65	6.00	4.97	5.72
Nd	18.70	16.50	18.30	19.50	16.20	19.10
Sm	2.95	2.63	2.83	3.05	2.62	2.88
Eu	0.69	0.66	0.68	0.67	0.72	0.65
Gd	2.34	2.07	2.16	2.30	2.18	2.26
Tb	0.35	0.32	0.32	0.34	0.39	0.34
Dy	1.97	1.89	1.70	1.76	2.02	1.71
Ho	0.43	0.42	0.36	0.38	0.50	0.37
Er	1.47	1.37	1.29	1.22	1.47	1.17
Tm	0.22	0.23	0.19	0.19	0.29	0.20
Yb	1.54	1.56	1.37	1.38	1.72	1.40
Lu	0.25	0.25	0.22	0.22	0.33	0.24
Y	12.70	12.10	11.10	11.40	12.80	11.20
Cs	5.24	5.08	5.49	6.11	5.28	5.69
Ta	1.83	2.05	1.36	1.35	2.21	1.02
Hf	3.60	3.60	3.41	3.51	3.59	4.26
Ga	12.70	12.40	13.00	12.90	12.70	12.80
Zn	25.70	20.70	17.10	17.40	18.60	16.40
Pb	17.30	16.70	16.10	14.70	18.10	15.40
ΣREE	119.17	107.04	118.28	124.31	106.51	122.84
ΣLREE	110.60	98.93	110.66	116.52	97.61	115.15
ΣHREE	8.57	8.11	7.62	7.78	8.90	7.69
LREE/HREE	12.91	12.20	14.52	14.98	10.96	14.98
La_N/Yb_N	13.32	11.63	14.71	15.13	10.72	15.42
δEu	0.80	0.87	0.84	0.78	0.92	0.78

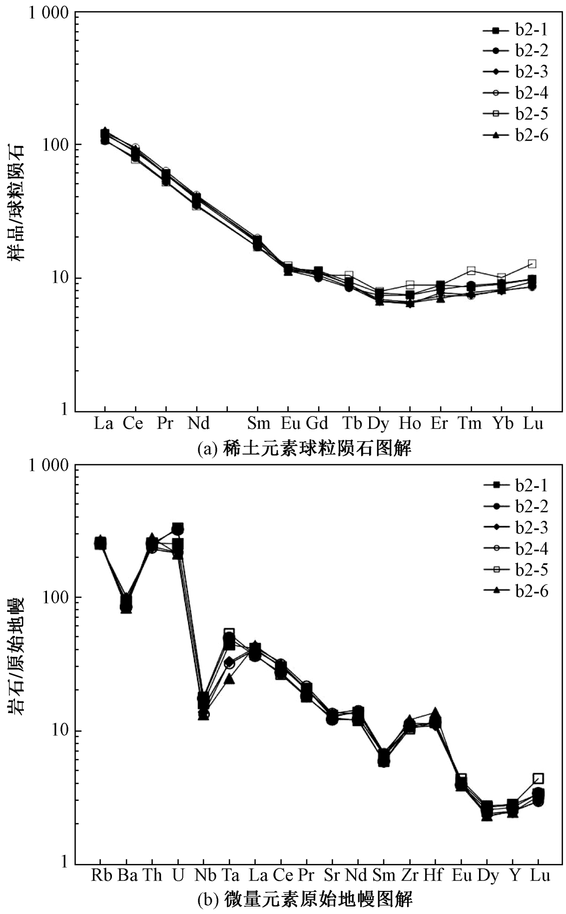

图6 长山二长花岗岩稀土元素球粒陨石图解和微量元素原始地幔图解[46]

Fig. 6 Chondrite-normalized rare earth element patterns and trace elements spider diagram of the Changshan monzogranite[46]

5 岩体成因及其形成的构造背景

5.1 成因类型

判断Ⅰ型、S型和A型花岗岩的关键且特异性高的矿物学标志为堇青石、角闪石及碱性铁镁矿物[47-49],根据检测结果判断出,岩石的矿物组分主要是钾长石、石英、黑云母等,副矿物有锆石、榍石等,同时不含有石榴子石、堇青石等,角闪石和黑云母表现出I型花岗岩的矿物成分特征[50]。

样品的 Zr+Nb+Ce+Y 含量均值为 200.19×10^{-6},低于A型花岗岩的下限(350×10^{-6})。根据图7相关结果可知,样品全部投入未分异的Ⅰ型花岗岩区域。样品 $K_2O/Na_2O>1$,与 Barbarin[51]划分的富钾钙碱性花岗岩(KCG)一致;显示了Ⅰ型花岗岩的岩石地球化学特征[52]。根据图6(b)结果可知,其微量元素相对富集大离子亲石元素、贫化高强场元素,表现出火山弧Ⅰ型花岗岩的特点[53],指示其源区为类似岛弧区的后碰撞花岗岩的物源[54-55]。综合分析,长山地区二长花岗岩属于高钾-

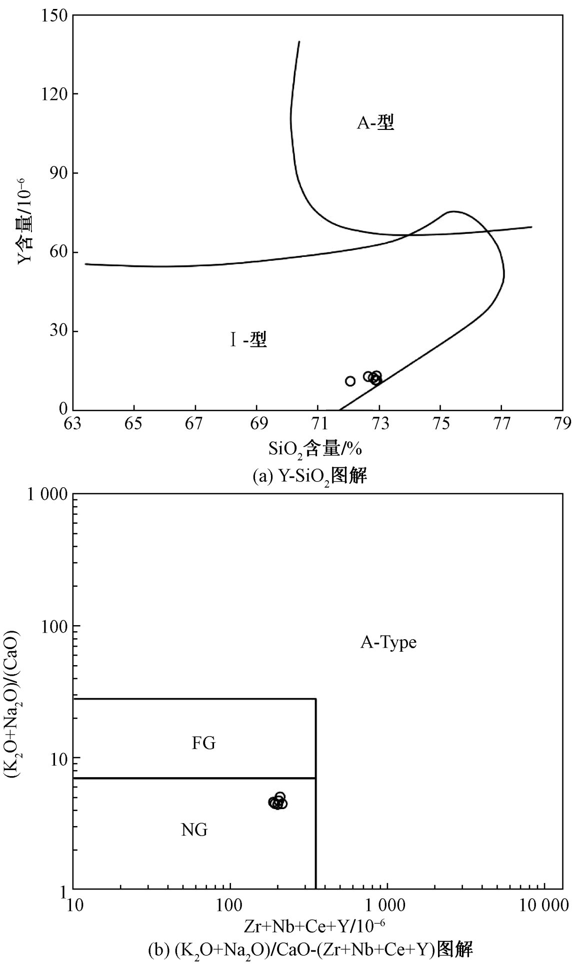

A-type 为 A 型花岗岩;FG 为分异的长英质花岗岩;
NG 为正常(未分异)的 M、I 和 S 型花岗岩

图 7　长山二长花岗岩成因类型判别图解[44,56]

Fig. 7　Diagrammatic diagram of genetic types of the Changshan monzogranite[44,56]

钾玄质钙碱性、过铝质 I 型花岗岩。

5.2　构造环境及地质意义

长山二长花岗岩具有轻重稀土分馏较弱以及 Eu 异常较弱的稀土元素特征,由此可判断出大部分岩体在岩浆演化中存在一定程度的斜长石的结晶分离现象[45,57],样品在 A/CNK-A/NK 图解中显示过铝质花岗岩特征[图 5(d)],与玄武质岩浆在结晶分异时的过碱性花岗岩明显不同[58-59]。

样品的 Zr/Hf 为 31.92 ~36.47,中值 33.95,与壳源的 Zr/Hf 近似,在微量元素原始地幔标准化图解上显示 Ba、Nb 显著负异常和 Zr、Hf 正异常的特征[60];样品的 La/Nb 比值为 2.01 ~2.49,偏向于地壳的相应比值[61],样品的 Nb/Ta 比值为 5.79 ~9.28,与原始地幔形成的岩石相比[62](Nb/Ta =17.6),岩体更可能为中下地壳熔融成因[63](Nb/Ta =12.4)。

已研究表明地壳部分熔融成因的岩浆显示低 Al_2O_3、MgO、Cr、Ni,高 K_2O 的特征[64],长山二长花岗的 Cr 含量为 2.36×10^{-6} ~ 4.79×10^{-6},Ni 含量为 0.83×10^{-6} ~ 25.0×10^{-6},较低的 Al_2O_3、$Mg^{\#}$、Cr、Ni 以及较高的 K_2O 的含量,由此可判断出其岩浆可能为地壳岩石的部分熔融的产物,样品高 Sr/Y、低 Yb、HREE 亏损的特征指示源区存在石榴石、角闪石的残留相,角闪石、石榴石残留相的稳定受压力制约,由此可以反映源区的地壳厚度[65],长山二长花岗岩表现为 HREE 轻微上凹的稀土配分特征[图 6(b)],且 Y/Yb 为 7.44 ~8.26,总体接近 10,Sm/Yb 介于 1.52 ~2.2,总体小于 4,Dy/Yb 介于 1.17 ~1.28,总体小于 2,指示其岩体成因可能为中下地壳来源[66-68]。

研究区花岗岩体缺乏详细的 Sr-Nd 同位素资料,导致不能对长山二长花岗岩的源岩或成因模式进行准确的限制;另外,长山地区岩体亏损 Nb,进一步表明不可能由地幔基性岩浆结晶分异形成[69]。

从图 8 可知,样品落入埃达克岩与经典岛弧岩的交界区域,样品的 Sr 的含量为 258×10^{-6} ~286 ×

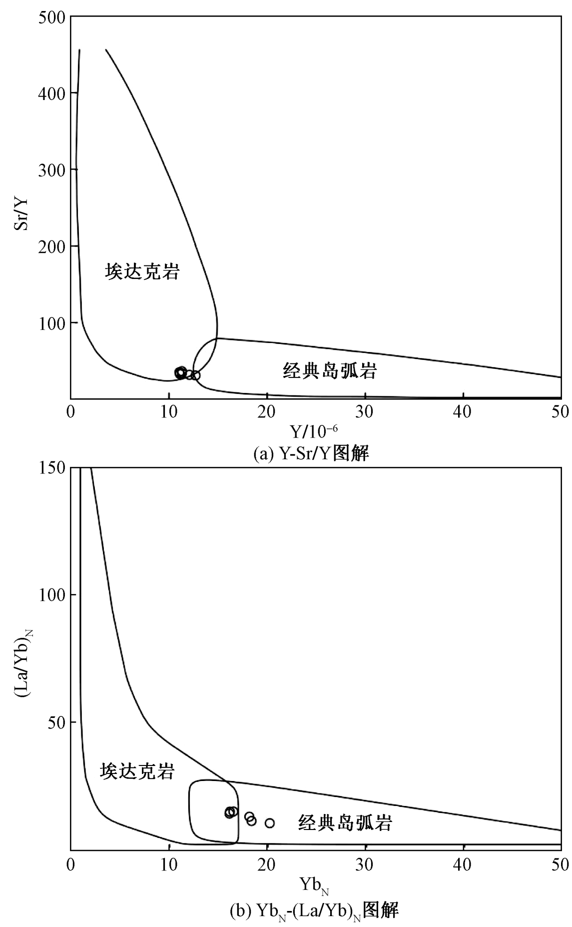

图 8　长山二长花岗岩 Y-Sr/Y 图解和 Yb_N-$(La/Yb)_N$ 图解[77]

Fig. 8　Y-Sr/Y and Yb_N-$(La/Yb)_N$ diagrammatic diagrams of the Changshan monzogranite[77]

10^{-6},Y 的含量为 $11.1\times10^{-6}\sim12.8\times10^{-6}$,Yb 的含量为 $1.37\times10^{-6}\sim1.72\times10^{-6}$,Sr/Y 为 20.78 ~ 25.41,La/Yb 为 14.94 ~ 21.50。其高硅($SiO_2>56\%$)、低镁($MgO<3\%$)、低 Y($Y<20\times10^{-6}$)、低 Yb($Yb<2\times10^{-6}$)、高 Sr/Y(Sr/Y >20)、高 La/Yb(La/Yb >7.6)且亏损 HREE、富集 LILE、亏损 HFSE 的特点表现出与代表俯冲环境的典型埃达克岩相似的地球化学特征,但与在俯冲挤压环境中地幔玄武岩结晶分异形成的具有富 Na($K_2O/Na_2O<1$)、富 Mg($Mg^{\#}>40$)且高 Sr($Sr>400\times10^{-6}$)的典型埃达克岩不同,长山二长花岗岩表现出富 K,低 Mg 且低 Sr 低 Yb 的地球化学特征,这类富钾钙碱性花岗岩在现今的喜马拉雅-古特提斯构造域广泛分布,其形成于后碰撞构造环境中下地壳的部分熔融[70-76]。

在花岗岩构造环境判别图解上[44,78][图 9],样品均落入后碰撞花岗岩区域,指示长山二长花岗岩

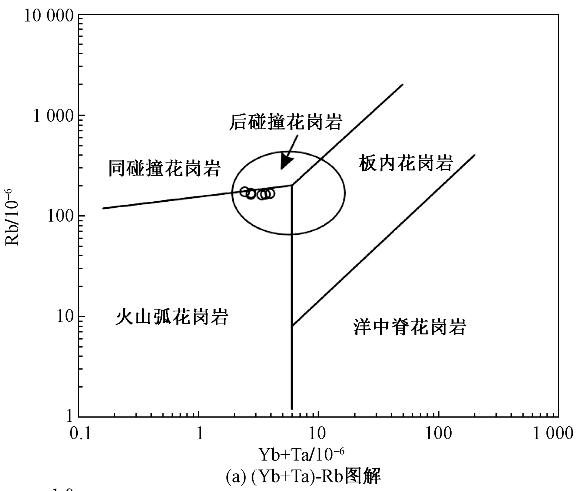

(a) (Yb+Ta)-Rb图解

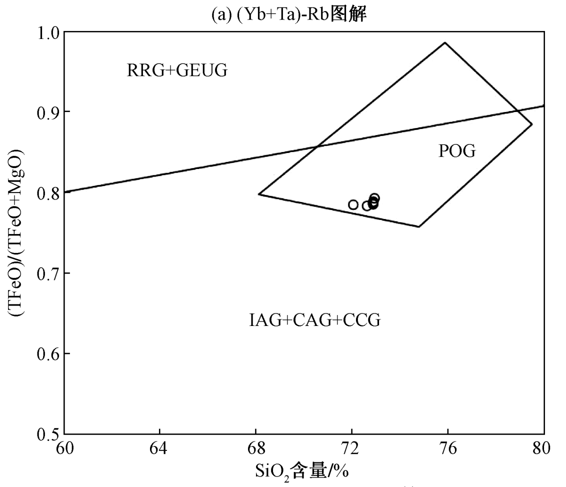

(b) SiO_2-TFeO/(TFeO+MgO)图解

IAG 为岛弧花岗岩类;CAG 为大陆弧花岗岩;CCG 为大陆碰撞花岗岩;POG 为后碰撞花岗岩;RRG 为与裂谷有关的花岗岩;CEUG 为与大陆的造陆抬升有关的花岗岩

图 9 长山二长花岗岩构造环境判别图解[44,78]

Fig. 9 Diagrammatic diagram of tectonic environment of the Changshan monzogranite[44,78]

可能是早二叠世后碰撞构造环境中下地壳部分熔融的产物,其形成过程与“喜马拉雅型花岗岩”相同,在大陆造山带碰撞后岩石圈松弛阶段状态转折时往往伴随着强烈的岩浆活动,花岗岩物质来源为富钾的中下地壳的部分熔融,富钾钙碱性花岗岩的大量产出[59,79]。

综上所述,北山南带长山二长花岗岩在后碰撞构造环境中下地壳岩石部分熔融形成并最终侵位的高钾钙碱性花岗岩。

6 结论

(1)北山南带长山二长花岗岩中锆石 LA-ICP-MS U-Pb 年龄为(291.1 ± 1.5) Ma,为早二叠世岩浆活动产物,与北山地区早二叠世岩浆活动时间一致。

(2)长山二长花岗岩为高钾钙碱性、过铝质 I 型花岗岩;岩石样品稀土元素总含量为 $106.51\times10^{-6}\sim124.31\times10^{-6}$,且轻/重稀土的比值变化范围为 10.96 ~ 14.98(平均值为 13.43),指示轻稀土相对重稀土富集。Eu 弱负异常。样品富集大离子亲元素、贫化高场强元素。

(3)结合区域构造演化模式,认为北山南带长山地区二长花岗岩形成于后碰撞构造环境中下地壳部分熔融的产物。

参 考 文 献

[1] Yakubchuk A. Architecture and mineral deposit settings of the Altaid orogenic collage: a revised model[J]. Journal of Asian Earth Sciences, 2004, 23(5): 761-779.

[2] 耿全如, 李文昌, 王立全, 等. 特提斯中西段古生代洋陆格局与构造演化[J]. 沉积与特提斯地质, 2021, 41(2): 297-315.
Geng Quanru, Li Wenchang, Wang Liquan, et al. Paleozoic tectonic framework and evolution of the central and western Tethys[J]. Sedimentary Geology and Tethyan Geology, 2021, 41(2): 297-315.

[3] Cawood P A, Kroner A, Collins W J, et al. Earth accretionary orogens through Earth history[C]//Cawood P A, Kroner A. Earth Accretionary Systems in Space and Time. Geological Society. London: Special Publications, 2009: 1-36.

[4] 计文化, 李荣社, 陈奋宁, 等. 中国西北地区南华纪—古生代构造重建及关键问题讨论[J]. 地质力学学报, 2020, 26(5): 634-655.
Ji Wenhua, Li Rongshe, Chen Fenning, et al. Tectonic reconstruction of northwest China in the Nanhua-Paleozoic and discussions on key issues[J]. Journal of Geomechanics, 2020, 26(5): 634-655.

[5] 高俊, 江拓, 王信水, 等. 准噶尔—天山—北山蛇绿岩: 对中亚造山带西南缘洋陆格局演化的制约[J]. 地质科学, 2022, 57(1): 1-42.
Gao Jun, Jiang Tuo, Wang Xinshui, et al. The Junggar, Tianshan and Beishan ophiolites: constraint on the evolution of oceanic and continental framework along the southwestern margin of the Central-

Asian Orogenic Belt[J]. Chinese Journal of Geology, 2022, 57(1): 1-42.

[6] 张旗, 周国庆. 中国蛇绿岩[M]. 北京: 科学出版社, 2001.
Zhang Qi, Zhou Guoqing. Ophiolites of China[M]. Beijing: Science Press, 2001.

[7] 方维萱, 郑小明, 方同辉, 等. 甘肃红石山地区泥盆纪—石炭纪有限洋盆重建与蛇绿混杂岩深部结构[J]. 地质通报, 2021, 40(5): 649-673.
Fang Weixuan, Zheng Xiaoming, Fang Tonghui, et al. Restoration of the Devonian-Carboniferous limited ocean basin and deep structure of ophiolitic melange in the Hongshishan area of Gansu Province[J]. Geological Bulletin of China, 2021, 40 (5): 649-673.

[8] 何碧, 赵振瑄, 刘海生, 等. 东天山造山带黑尖山地区花岗闪长岩岩石成因及构造意义: 来自岩石学、锆石 U-Pb 年代学、地球化学证据[J]. 科学技术与工程, 2024, 24(25): 10620-10634.
He Bi, Zhao Zhenguan, Liu Haisheng, et al. Petrogenesis and tectonic significance of late devonian granodiorite in Heijinshan area, eastern Tianshan orogenic belt: evidences from petrology, zircon U-Pb geochronology, and geochemistry[J]. Science Technology and Engineering, 2024, 24(25): 10620-10634.

[9] Xiao W J, Mao Q G, Windley B F, et al. Paleozoic multiple accretionary and collisional processes of the Beishan orogenic collage[J]. American Journal of Science, 2010, 310(10): 1553-1594.

[10] He Z Y, Klemd R, Yan L L, et al. The origin and crustal evolution of microcontinents in the Beishan orogen of the southern Central Asian Orogenic Belt[J]. Earth-Science Reviews, 2018, 185: 1-14.

[11] 宋东方, 肖文交, 韩春明, 等. 北山中部增生造山过程: 构造变形和 ^{40}Ar-^{39}Ar 年代学制约[J]. 岩石学报, 2018, 34(7): 2087-2098.
Song Dongfang, Xiao Wenjiao, Han Chunming, et al. Accretionary processes of the central segment of Beishan: constraints from structural deformation and ^{40}Ar-^{39}Ar geochronology[J]. Acta Petrologica Sinica, 2018, 34(7): 2087-2098.

[12] 何世平, 周会武, 任秉琛, 等. 甘肃内蒙古北山地区古生代地壳演化[J]. 西北地质, 2005, 38(3): 6-15.
He Shiping, Zhou Huiwu, Ren Bingchen, et al. Crustal evolution of Palaeozoic in Beishan area, Gansu and Inner Mongolia, China[J]. Northwestern Geology, 2005, 38(3): 6-15.

[13] 聂凤军, 江思宏, 白大明, 等. 北山地区金属矿床成矿规律及找矿方向[M]. 北京: 地质出版社, 2002.
Nie Fengjun, Jiang Sihong, Bai Daming, et al. Metallogenic studies and ore prospecting in the Conjunction Area of Inner Mongollutonomous Region, Gansu Province and Xinjiang Uygur Autonomous Region (Beishan Mt.), northwest China[M]. Beijing: Geological Publishing House, 2002.

[14] Zheng R, Wu T, Zhang W, et al. Geochronology and geochemistry of late Paleozoic magmatic rocks in the Yinwaxia area, Beishan: implications for rift magmatism in the southern Central Asian Orogenic Belt[J]. Journal of Asian Earth Sciences, 2014, 91: 39-55.

[15] 陈杰, 赵吉昌, 杨镇熙, 等. 甘肃北山红旗山井岩体锆石 U-Pb 定年、地球化学特征及地质意义[J]. 科学技术与工程, 2024, 24(25): 10688-10700.
Chen Jie, Zhao Jichang, Yang Zhenxi, et al. Zircon U-Pb dating, geochemical characteristics and geological significance of Hongqishanjing rock mass from Beishan area, Gansu Province[J]. Science Technology and Engineering, 2024, 24(25): 10688-10700.

[16] Zhang Y, Dostal J, Zhao Z, et al. Geochronology, geochemistry and petrogenesis of mafic and ultramafic rocks from Southern Beishan Area, NW China: implications for crust-mantle interaction[J]. Gondwana Research, 2011, 20(4): 816-830.

[17] 王盛栋. 甘肃北山中部地区古生代洋板块地层重建与构造演化[D]. 武汉: 中国地质大学, 2017.
Wang Shengdong. Reconstruction of paleozoic ocean plate stratigraphy in the middle Beishan Area, Gansu Province[D]. Wuhan: China University of Geosciences, 2017.

[18] 过磊, 王国强, 郭琳, 等. 北山造山带南部芦草沟地区早三叠世酸性脉岩成因[J]. 矿物岩石地球化学通报, 2018, 37(3): 502-512.
Guo Lei, Wang Guoqiang, Guo Lin, et al. Petrogenesis of early triassic felsic dikes in the Lucaogou Area of southern Beishan Orogenic Belt[J]. Bulletin of Mineralogy, Petrology and Geochemistry, 2018, 37(3): 502-512.

[19] 左国朝, 刘义科, 李绍雄. 甘肃省北山地区罗雅楚山—大红山一带区域构造格局、褶皱样式及断裂系[J]. 甘肃地质, 2011, 20(1): 6-15.
Zuo Guochao, Liu Yike, Li Shaoxiong. Tectonic framework, fold styles and fault systems of Luoyachusha-Dahongshan area in Beishan region of Gansu Province[J]. Gansu Geology, 2011, 20(1): 6-15.

[20] 吕鑫, 于晓飞, 杜泽忠, 等. 甘肃北山南带晚泥盆世岩浆事件: 锆石 U-Pb 年代学、地球化学和 Sr-Nd-Hf 同位素体系约束[J]. 岩石学报, 2022, 38(3): 693-712.
Lü Xin, Yu Xiaofei, Du Zezhong, et al. Late devonian magmatic event in the South Beishan orogenic belt, Gansu: constraints from zircon U-Pb chronology, geochemistry and Sr-Nd-Hf isotopes[J]. Acta Petrologica Sinica, 2022, 38(3): 693-712.

[21] 王国强, 李向民, 徐学义, 等. 北山造山带古生代蛇绿混杂岩研究现状及进展[J]. 地质通报, 2021, 40(1): 71-81.
Wang Guoqiang, Li Xiangmin, Xu Xueyi, et al. Research status and progress of Paleozoic ophiolites in Beishan orogenic belt[J]. Geological Bulletin of China, 2021, 40(1): 71-81.

[22] 黄博涛, 王国强, 王居里, 等. 北山造山带破城山地区冰碛岩沉积时代、物源及构造意义: 来自碎屑锆石 U-Pb 年代学及 Lu-Hf 同位素的约束[J]. 地质学报, 2023, 97(10): 3213-3224.
Huang Botao, Wang Guogiang, Wang Juli, et al. Sedimentary age, provenance and tectonicimplications of the diamictite in Pochengshan Area, Beishan: Constraints from detrital zircon U-Pb dating and Hf isotope[J]. Acta Geologica Sinica, 2023, 97(10): 3213-3224.

[23] 毛启贵, 肖文交, 韩春明, 等. 北山柳园地区中志留世埃达克质花岗岩类及其地质意义[J]. 岩石学报, 2010, 26(2): 584-596.
Mao Qigui, Xiao Wenjiao, Han Chunming, et al. Discovery of Middle Silurian adakitegranite and its tectonic significance in Liuyuan Area, Beishan Moutains, NW China[J]. Acta Petrologica Sinica, 2010, 26(2): 584-596.

[24] Zhu J, Lü X, Peng S. U-Pb zircon geochronology, geochemistry and tectonic implications of the early Devonian granitoids in the

Liuyuan Area, Beishan, NW China[J]. Geosciences Journal, 2016, 20: 609-625.

[25] 王疆涛, 董云鹏, 曾忠诚, 等. 北山造山带南部黄草滩岩体年代学、地球化学及地质意义[J]. 现代地质, 2016, 30(5): 937-949.
Wang Jiangtao, Dong Yunpeng, Zeng Zhongcheng, et al. Geochronology, geochemistry and geological significance of the Huangcaotan Pluton in the Southern Beishan Orogenic Belt[J]. Geoscience, 2016, 30(5): 937-949.

[26] 左国朝, 刘义科, 刘春燕. 甘新蒙北山地区构造格局及演化[J]. 甘肃地质学报, 2003, 12(1): 1-5.
Zuo Guochao, Liu Yike, Liu Chunyan. Framework and evolution of the tectonic structure in structure in Beishan Area across Gansu Province, Xinjiang Autonomous region and inner Mongolia Autonomous Region[J]. Acta Geologica Gansu, 2003, 12(1): 1-5.

[27] 赵泽辉, 郭召杰, 王毅. 甘肃北山柳园地区花岗岩类的年代学, 地球化学特征及构造意义[J]. 岩石学报, 2007, 23(8): 1847-1860.
Zhao Zehui, Guo Zhaojie, Wang Yi. Geochronology, geochemical characteristics and tectonic implications of the granitoids from Liuyuan area, Beishan, Gansu Province, northwest China[J]. Acta Petrologica Sinica, 2007, 23(8): 1847-1860.

[28] 杨合群, 李英, 李文明, 等. 2008. 北山成矿构造背景概论[J]. 西北地质, 2008, 41(1): 22-28.
Yang Hequn, Li Ying, Li Wenming, et al. General discussion on metallogenitic tectonic setting of Beishan Mountain[J]. Northwestern China, 2008, 41(1): 22-28.

[29] 许伟, 徐学义, 牛亚卓, 等. 北山南部早二叠世A型流纹岩地球化学特征及其地球动力学意义[J]. 岩石学报, 2018, 34(10): 3011-3033.
Xu Wei, Xu Xueyi, Niu Yazhuo, et al. Geochronology, petrogenesis and tectonic implications of Early Permian A-type rhyolite from southern Beishan orogen, NW China[J]. Acta Petrologica Sinica, 2018, 34(10): 3011-3033.

[30] 卜涛, 余吉远, 过磊, 等. 甘肃北山大豁落南地区晚二叠世花岗闪长岩成因—锆石U-Pb年龄和岩石地球化学制约[J]. 地质通报, 2019, 38(2/3): 254-265.
Bu Tao, Yu Jiyuan, Guo Lei, et al. Petrogenesis of the Late Permian granodiorite in southern Dahuoluo Area, Beishan, Gansu: Constraints from zircon U-Pb geochronology and geochemistry[J]. Geological Bulletin of China, 2019, 38(2/3): 254-265.

[31] 孙海瑞, 吕志成, 于晓飞, 等. 甘肃柳园地区早二叠世正长花岗斑岩脉锆石U-Pb年代学、岩石地球化学特征—对北山造山带晚古生代构造背景的指示[J]. 吉林大学学报(地球科学版), 2020, 50(5): 1433-1449.
Sun Hairui, Lü Zhicheng, Yu Xiaofei, et al. Late Paleozoic tectonic evolution of Beishan orogenic belt: chronology and geochemistry constraints of Early Permian Syenogranitic Porphyry Dyke in Liuyuan Area, Gansu Province[J]. Journal of Jilin University (Earth Science Edition), 2020, 50(5): 1433-1449.

[32] 赵宏刚, 梁积伟, 王驹, 等. 甘肃北山南带沙枣园复式岩体年代学、地球化学特征及其构造意义[J]. 地质学报, 2020, 94(2): 396-425.
Zhao Honggang, Liang Jiwei, Wang Ju, et al. Geochronology, geochemical characteristies and tectonie significance of the Shazaoyuan Composite Pluton in the southern Beishan Mountains, Gansu Province, China[J]. Acta Geologica Sinica, 2020, 94(2): 396-425.

[33] 张文, 冯继承, 郑荣国, 等. 甘肃北山音凹峡南花岗岩体的锆石LA-ICP-MS定年及其构造意义[J]. 岩石学报, 2011, 27(6): 1649-1661.
Zhang Wen, Feng Jicheng, Zheng Rongguo, et al. LA-ICP-MS zircon U-Pb ages of the granites from the south of Yin'aoxia and their tectonic significances[J]. Acta Petrologica Sinica, 2011, 27(6): 1649-1661.

[34] 董洪凯, 薛鹏远, 刘广, 等. 内蒙古北山地区芨芨台子—小黄山蛇绿岩构造属性及与成矿关系: 来自阿民乌素地幔橄榄岩印证[J]. 地质与勘探, 2022, 58(4): 767-777.
Dong Hongkai, Xue Pengyuan, Liu Guang, et al. Tectonic attributes of the Jijitaizi-Xiaohuangshan ophiolite in the Beishan Area, Inner Mongolia and in relationship to metallogenesis: evidence from the Aminwusu mantle peridotite[J]. Geology and Exploration, 2022, 58(4): 767-777.

[35] 江思宏, 聂凤军. 北山地区花岗岩类的$^{40}Ar/^{39}Ar$同位素年代学研究[J]. 岩石学报, 2006, 22(11): 2719-2732.
Jiang Sihong, Nie Fenjun. $^{40}Ar/^{39}Ar$ geochronology of the granitoids in Beishan Mountain, NW China[J]. Acta Petrologica Sinica, 2006, 22(11): 2719-2732.

[36] 杨镇熙, 赵青虎, 张晶, 等. 甘肃北山地区黑山头石英二长闪长岩年代学、地球化学特征及其地质意义[J]. 矿物岩石地球化学通报, 2022, 41(6): 1165-1177.
Yang Zhenxi, Zhao Qinghu, Zhang Jing, et al. Chronological and geochemical characteristics of the Heishantou Quartz-monzodiorite in the Beishan Area, Gansu Province, China, and their geological significances[J]. Bulletin of Mineralogy, Petrology and Geochemistry, 2022, 41(6): 1165-1177.

[37] 冯继承, 张文, 吴泰然, 等. 甘肃北山桥湾北花岗岩体的年代学、地球化学及其地质意义[J]. 北京大学学报(自然科学版), 2012, 48(1): 61-70.
Feng Jicheng, Zhang Wen, Wu Tairan, et al. Geochronology and geochemistry of granite pluton in the north of Qiaowan, Beishan Mountain, Gansu Province, China, and its geological significance[J]. Acta Scientiarum Naturalium Universitatis Pekinensis, 2012, 48(1): 61-70.

[38] 吴元保, 郑永飞. 锆石成因矿物学研究及其对U-Pb年龄解释的制约[J]. 科学通报, 2004, 49(16): 1589-1604.
Wu Yuanbao, Zheng Yongfei. Genesis of zircon and its constraints on interpretation of U-Pb age[J]. Chinese Science Bulletin, 2004, 49(16): 1589-1604.

[39] 李长民. 锆石成因矿物学与锆石微区定年综述[J]. 地质调查与研究, 2009, 33(3): 161-174.
Li Changmin. A review on the minerageny and situmicroanalytical dating techniques of Zircons[J]. Geological Survey and Research, 2009, 33(3): 161-174.

[40] Harley S L, Kelly N M. Zircon: tiny but timely[J]. Elements, 2007, 3(1): 3-18.

[41] De la Roche H D, Leterrier J T, Grandclaude P, et al. A classification of volcanic and plutonic rocks using R1R2-diagram and major-element analysesits relationships with current nomenclature[J]. Chemical geology, 1980, 29(1/4): 183-210.

[42] Wright J B. A simple alkalinity ratio and its application to questions of non-orogenic granite genesis[J]. Geological Magazine,

1969, 106(4): 370-384.

[43] Middlemost E A K. Magmas and magmatic rocks: an introduction to igneous petrology [M]. London: Addison-Wesley Longman Ltd., 1985.

[44] Maniar P D, Piccoli P M. Tectonic discrimination of granitoids [J]. Geological Society of America Bulletin, 1989, 101(5): 635-643.

[45] Henderson P. Inorganie geochemistry[M]. New York: Pergamon Press, 1982.

[46] Sun S S, McDonough W F. Chemical and isotopic systematics of oceanic basalts: implications for mantle composition and processes [M]//Saunders A D, Norry M J. Magmatism in the Ocean Basins. Geological Society. London: Special Publications, 1989.

[47] 吴福元, 李献华, 杨进辉, 等. 花岗岩成因研究的若干问题[J]. 岩石学报, 2007, 23(6): 1217-1238.
Wu Fuyuan, Li Xianhua, Yang Jinhui, et al. Discussions on the petrogenesis of granites[J]. Acta Petrologica Sinica, 2007, 23(6): 1217-1238.

[48] 刘龙, 张树明, 张鑫. 相山高分异 A 型花岗岩的识别及地质意义[J]. 科学技术与工程, 2022, 22(1): 57-64.
Liu Long, Zhang Shuming, Zhang Xin. Identification of highly differentiated A-type granite in Xiangshan and its geological significance[J]. Science Technology and Engineering, 2022, 22(1): 57-64.

[49] 李彦强, 雷勇亮, 刘松林, 等. 武夷地块黎川铝质 A 型花岗岩成因及其地质意义[J]. 科学技术与工程, 2023, 23(3): 953-964.
Li Yanqiang, Lei Yongliang, Liu Songlin, et al. Genesis and geological significance of aluminous A-type granite in Lichuan area, Wuyi block[J]. Science Technology and Engineering, 2023, 23(3): 953-964.

[50] Sylvester P J. Post-collisional strongly peraluminous granites[J]. Lithos, 1998, 45(1/4): 29-44.

[51] Barbarin B. A review of the relationships between granitoid types, their origins and their geodynamic environments [J]. Lithos, 1999, 46(3): 605-626.

[52] Chappell B W, White A J. I-and S-type granites in the Lachlan fold belt[J]. Earth and Environmental Science Transactions of the Royal Society of Edinburgh, 1992, 83(1/2): 1-26.

[53] Roberts M P, Clemens J D. Origin of high-potassium, calc-alkaline, I-type granitoids[J]. Geology, 1993, 21(9): 825-828.

[54] Kelemen P B, Johnson K T M, Kinzler R J, et al. High-field-strength element depletions in arc basalts due to mantle-magma interaction[J]. Nature, 1990, 345(6275): 521-524.

[55] Stolz A J, Jochum K P, Spettel B, et al. Fluid-and melt-related enrichment in the subarc mantle: evidence from Nb/Ta variations in island-arc basalts[J]. Geology, 1996, 24(7): 587-590.

[56] Collins W J, Beams S D, White A J, et al. Nature and origin of A-type granites with particular reference to southeastern Australia [J]. Contributions to Mineralogy and Petrology, 1982, 80: 189-200.

[57] 张旗, 潘国强, 李承东, 等. 花岗岩结晶分离作用问题——关于花岗岩研究的思考之二[J]. 岩石学报, 2007, 23(6): 1239-1251.
Zhang Qi, Pan Guoqiang, Li Chengdong, et al. Does fractional crystallization occur in granitic magma? some crucial questions on granite study(2)[J]. Acta Petrologica Sinica, 2007, 23(6): 1239-1251.

[58] Litvinovsky B A, Jahn B M, Zanvilevich A N, et al. Petrogenesis of syenite-granite suites from the Bryansky Complex (Transbaikalia, Russia): implications for the origin of A-type granitoid magmas[J]. Chemical Geology, 2002, 189(1/2): 105-133.

[59] 张旗, 潘国强, 李承东, 等. 花岗岩混合问题: 与玄武岩对比的启示——关于花岗岩研究的思考之一[J]. 岩石学报, 2007, 23(5): 1141-1152.
Zhang Qi, Pan Guoqiang, Li Chengdong, et al. Granitic magma mixing versus basaltic magma mixing: new viewpoints on granitic magma mixing process: some crucial questions on granite study (1)[J]. Acta Petrologica Sinica, 2007, 23(5): 1141-1152.

[60] Condie K C. Geochemical changes in baslts and andesites across the Archean-Proterozoic boundary: identification and significance [J]. Lithos, 1989, 23(1/2): 1-8.

[61] Depaolo D J, Daley E E. Neodymium isotopes in basalts of the Southwest Basin and range and lithospheric thinning during continental extension [J]. Chemical Geology, 2000, 169(1): 157-185.

[62] Hofmann A W. Chemical differentiation of the earth: the relationship between mantle, continental crust, and oceanic crust[J]. Earth and Planetary Science Letters, 1988, 90(3): 297-314.

[63] Rudnick R L, Gao S. Composition of the continental crust[M]. Oxford: Treatise on Geochemistry, Pergamon, 2003.

[64] Atherton M P, Petford N. Generation of sodium-rich magmas from newly underplated basaltic crust[J]. Nature, 1993, 362(64): 144-166.

[65] Xiong X L, Adam J, Green T H. Rutile stability and rutile/melt HFSE partitioning during partial melting of hydrous basalt: implications for TTG genesis[J]. Chemical Geology, 2005, 218(3/4): 339-359.

[66] Mamani M, Wörner G, Sempere T. Geochemical variations in igneous rocks of the Central Andean orocline (13 S to 18 S): tracing crustal thickening and magma generation through time and space[J]. Bulletin, 2010, 122(1/2): 162-182.

[67] 张竞嘉, 云龙, 田霄, 等. 北山南带新场岩体地球化学特征及构造意义[J]. 世界核地质科学, 2021, 38(2): 250-261.
Zhang Jingjia, Yun Long, Tian Xiao, et al. Geochemical characteristics of Xinchang pluton in southern Beishan and its tectonic significance[J]. World Nuclear Geoscience, 2021, 38(2): 250-261.

[68] 俞胜, 赵斌斌, 贾轩, 等. 北山造山带南缘一条山北闪长岩地球化学, 年代学特征及其构造意义[J]. 西北地质, 2022, 55(4): 267-279.
Yu Sheng, Zhao Binbin, Jia Xuan, et al. Geochemistry, geochronology characteristics and tectonic significance of Yitiaoshan Dioritein the Southern Margin of Beishan Orogenic Belt[J]. Northwestern Geology, 2022, 55(4): 267-279.

[69] Green T H. Significance of Nb/Ta as an indicator of geochemical processes in the Crust-Mantle system[J]. Chemical Geology, 1995, 120(3/4): 347-359.

[70] Chung S L, Liu D, Ji J, et al. Adakites from continental collision zones: melting of thickened lower crust beneath southern Tibet [J]. Geology, 2003, 31(11): 1021-1024.

[71] Hou Z Q, Gao Y F, Qu X M, et al. Origin of adakitic intrusives

generated during mid-Miocene east-west extension in southern Tibet[J]. Earth and Planetary Science Letters, 2004, 220(1/2): 139-155.

[72] Moyen J F. High Sr/Y and La/Yb ratios: the meaning of the "adakitic signature"[J]. Lithos, 2009, 112(3/4): 556-574.

[73] Han B F, Guo Z J, Zhang Z C, et al. Age, geochemistry, and tectonic implications of a late Paleozoic stitching pluton in the North Tian Shan suture zone, western China[J]. Geological Society of American Bulletin, 2010, 122: 627-640.

[74] 张旗, 王元龙, 金惟俊, 等. 造山前, 造山和造山后花岗岩的识别[J]. 地质通报, 2008, 27(1): 1-18.
Zhang Qi, Wang Yuanlong, Jin Weijun, et al. Criteria for the recognition of pre, syn-and post-orogenic granitic rocks[J]. Geological Bulletin of China, 2008, 27(1): 1-18.

[75] 张旗, 焦守涛. 埃达克岩来自高压背景——一个科学的、可靠的、有预见性的科学发现[J]. 岩石学报, 2020, 36(6): 1675-1683.
Zhang Qi, Jiao Shoutao. Adakite comes from a high-pressure background: a scientific, reliable, predictable scientific discovery[J]. Acta Petrologica Sinica, 2020, 36(6): 1675-1683.

[76] 陈艺超, 张继恩, 候全林, 等. 增生弧基本特征与地质意义[J]. 地质科学, 2021, 56(2): 615-634.
Chen Yichao, Zhang Ji'en, Hou Quanlin, et al. The basic characteristics of accretion arcs and its geological implications[J]. Chinese Journal of Geology, 2021, 56(2): 615-634.

[77] Defant M J. Adakites: some variations on a theme[J]. Acta Petrologica Sinica, 1990, 18: 129-142.

[78] Pearce J A, Harris N B, Tindle A G. Trace element discrimination diagrams for the tectonic interpretation of granitic rocks[J]. Journal of Petrology, 1984, 25(4): 956-983.

[79] Rudnick R L. Making continental crust[J]. Nature, 1995, 378(6557): 571-578.